Histol Histopathol (2022) 37: 81-91

http://www.hh.um.es

Histology and Histopathology
From Cell Biology to Tissue Engineering

ORIGINAL ARTICLE **Open Access**

Upregulation of TLR9 may contribute to activation of microglia and painful diabetic neuropathy via the p38 MAPK pathway in rats

Zhaoxia Niu[1], Lei Bao[2] and Jing Chen[3]

[1]Department of Endocrinology, Jiaozhou Central Hospital of Qingdao, [2]Department of Endocrinology, Qingdao Chengyang People's Hospital and [3]Department of Gastroenterology and Endocrinology, Weifang Hanting District People's Hospital, Weifang City, Shandong Province, China

Summary. Painful diabetic neuropathy is a common chronic complication of diabetes, and the underlying mechanism remains largely elusive. A rat model of painful diabetic neuropathy was established via streptozotocin (STZ) injection and assessed as increased heat and mechanical hypersensitivity. An upregulation of TLR9 was observed in the spinal cords of rats injected with STZ and rat microglia (primary microglia and immortalized microglia HAPI) treated with high glucose. To investigate the role of TLR9 in high glucose-induced microglia activation, short hairpin RNAs targeting TLR9 were used *in vitro* to knock down TLR9 in HAPI cells. TLR9 interference suppressed the high glucose-induced expression and secretion of inflammatory cytokines (TNF-α, IL-1β, and IL-6), IBA-1 expression and the chemotaxis of HAPI microglia. Similar results were obtained when HAPI microglia were incubated with a p38 inhibitor (SB203580). P38 and ERK were downstream of TLR9 because TLR9 ablation markedly inhibited the phosphorylation of p38 and ERK. TLR9 was also knocked down *in vivo* via the injection of shTLR9 lentiviral vector into the rat spinal cord. Relief of STZ-induced heat and mechanical hypersensitivity was observed in rats with TLR9 interference, and TLR9 knockdown prevented STZ-induced inflammatory cytokine secretion and microglial and MAPK signaling activation. Our study revealed the participation of TLR9 in microglial activation and diabetes-induced hyperalgesia likely via the MAPK pathway. The targeting of TLR9 may be an effective strategy for the treatment of painful diabetic neuropathy.

Key words: Painful diabetic neuropathy, TLR9, Microglia activation, p38 MAPK

Corresponding Author: Jing Chen, Department of Gastroenterology and Endocrinology, Weifang Hanting District People's Hospital, No. 2600 Minzhu Street, Hanting District, Weifang City, Shandong Province, 261100, China. e-mail: Chenjjmedsci@163.com

DOI: 10.14670/HH-18-405

Introduction

Painful diabetic neuropathy is a common chronic complication of diabetes (diabetes mellitus) (Sloan et al., 2018), and it is one of the most common causes of acute or chronic pain syndrome in diabetic patients. Painful diabetic neuropathy primarily manifests as limb numbness and spontaneous neuralgia, hyperalgesia, and allodynia. The degree of pain varies from mild pain to stubborn severe pain that cannot be controlled by drugs. Diabetic neuropathy is a heavy burden on individuals and society (Wickramasinghe et al., 2016; Ebata-Kogure et al., 2017). The pathogenesis of painful diabetic neuropathy is complicated, and changes in inflammation and gene expression all lead to chronic pain (Castany et al., 2016; Sloan et al., 2018). Painful diabetic neuropathy is likely a combination of factors.

Glial cells in the spinal cord are responsible for the development and maintenance of neuropathic pain. Recent studies found that spinal microglia played an important role in the occurrence and development of painful diabetic neuropathy. Spinal microglia, but not astrocytes, are abnormally activated in streptozotocin (STZ)-induced diabetic rats (Tsuda et al., 2008). The activation of microglia is accompanied by the release of cytokines and the phosphorylation of mitogen-activated protein kinases (MAPKs), including p38-MAPK, extracellular signal-regulated kinase (ERK) and Jun N-terminal kinase (JNK). Activation of these pathways is related to the occurrence of pain hypersensitivity (Wang et al., 2014; Maruta et al., 2019). The inhibition of microglial activation is an important treatment strategy to reduce painful diabetic neuropathy (Zhang et al., 2018a-c; Zhong et al., 2018).

Toll-like receptor 9 (TLR9) belongs to the TLR family and is primarily involved in the regulation of innate immunity. Previous studies revealed a role of

Abreviations. STZ, streptozotocin; MAPK, mitogen-activated protein kinase; MWT, mechanical withdrawal thresholds; DM, Diabetes mellitus

TLR9 in some adaptive immunity-induced diseases (Silver et al., 2012). TLR9 also plays a role in regulating the inflammatory response and metabolism of non-immune cells. For example, mature neurons up-regulate the TLR9-AMPK signaling pathway in the presence of acute hypoxia to reduce cellular energy metabolism and improve survival (Oka et al., 2012; Shintani et al., 2013). TLR9 also plays a role in promoting chemotherapy-induced neuropathic pain (Luo et al., 2019). TLR9 is significantly upregulated in the retinas of diabetic rats (Jiang and Chen, 2017). The expression of TLR9 is up-regulated in neuronal cells treated with high glucose, and TLR9 knockdown reduces apoptosis and tau protein phosphorylation (Sun et al., 2017). However, the role and mechanism of TLR9 in painful diabetic neuropathy are not sufficiently understood. Our study established a rat model of painful diabetic neuropathy using a single injection of STZ, and our results revealed an increase in TLR9 expression in the hippocampus. Subsequent *in vitro* assays using rat primary microglia and the immortalized microglial cell line HAPI showed similar results. Knock down of TLR9 *in vitro* and *in vivo* demonstrated the role of TLR9 in the pathogenesis of painful diabetic neuropathy. Therefore, the targeting of TLR9 may be a therapeutic strategy for painful diabetic neuropathy.

Materials and methods

Animals and painful diabetic neuropathy model

The Ethical Committee of Jiaozhou Central Hospital of Qingdao approved all experimental procedures (No. 2020-03-003). Adult male Sprague-Dawley rats (175-200 g) were obtained from the Animal Laboratory Center (Shanghai, China). The experimental rats were fed a standard laboratory diet and housed under a 12-h light/dark cycle. The temperature was maintained at 23±2°C. Streptozotocin (STZ, Sigma, USA) was used to establish a painful diabetic neuropathy model, as widely acknowledged in previous research (Nasiry et al., 2017). After one week of adaptation to laboratory conditions, 60 rats were randomly divided into two groups, sham (n=30) and STZ (n=30) groups. After an overnight fast, a single intraperitoneal injection of STZ (50 mg/kg, freshly dissolved in citrate buffer) was administered to rats according to the method described in a previous study (Morrow, 2004). The sham group was given the same volume of citrate buffer. Seventy-two hours after STZ injection, tail vein blood was collected from the rats, and the blood glucose level was measured using a glucometer (One Touch Horizon, Johnson & Johnson, CA, USA). Rats with blood glucose levels above 16.7 mmol/l were considered diabetic, and rats with blood glucose levels below 16.7 mmol/l were excluded. Rats were continually fed a standard diet for three weeks after STZ administration, blood glucose and body weight were measured. Pain behaviors were assessed via measurement of mechanical and heat sensitivity to ensure the induction of a painful diabetic neuropathy model in rats.

Pain behavior assessments

For mechanical hypersensitivity measurement, the "up-down" method was applied using von Frey filaments (Lin et al., 2018; Oghbaei et al., 2020), with some modifications. Briefly, von Frey filaments with increasing stiffness (from 0.008 to 300 g) were applied, and the rats were placed in a plastic chamber for 30 min for adaptation before the test. The von Frey filaments were applied to the plantar surface of the hind paw for 5 sec. The maximum pressure was set as 30 g to avoid damage. The initial force selected was 0.4 g, and the force was increased (0.4, 0.6, 1.4, 2.0, 4.0, 6.0, 8.0, 15, and 26 g). If no withdrawal response was observed, a heavier force was applied. The force increased until an obvious withdrawal response occurred, and this value was recorded when at least three of five stimulations induced withdrawal responses. Each test was repeated three times with a 5-min interval between tests.

Thermal hyperalgesia was assessed according to a previous study with minimum modification (Huang et al., 2016). The rats were placed on a 2-mm thick glass floor and covered with a plexiglass box. A laser radiant heat source was positioned beneath the glass floor (Plantar Test Analgesia Meter 390G, IITC Life Science, CA, USA). Rat hind paws were stimulated with laser radiant heat at after 30 min of adaptation. A cut-off was set to 30 s to avoid tissue damage. Response latency was recorded when the heat stimulus induced a withdrawal response. Each test was repeated three times with a 5-min interval between tests.

Lentiviral vector and in vivo transfection

Two short hairpin RNAs (shRNAs) targeting rat TLR9 (shTLR9#1 and shTLR9#2) and a negative control shRNA were generated by GenePharma (Shanghai, China) and cloned into lentiviral vectors. For *in vivo* TLR9 lentiviral knockdown, rats (n=48, 12 per group) were randomly divided into four groups: sham, STZ, STZ+shNC, and STZ+shTLR9. Rats in the STZ, STZ+shNC, and STZ+shTLR9 groups were intraperitoneally injected with STZ as described above, and sham rats were injected with the same volume of citrate buffer. Two weeks after STZ injection, rats in the STZ+shNC and STZ+shTLR9 groups were anesthetized using 3% isoflurane (Abbott, USA) in oxygen, and the L4-L6 lumbar spinal cord was exposed. Ten microliters of lentivirus (against TLR9 or negative control, 1.0×10^7 TU/ml) was intrathecally injected into the L4 and L5 intervertebral space of the spinal cord using a Hamilton syringe with a 30-gage needle. Rats in the sham and STZ groups underwent the same surgery with no lentivirus delivery. The timeline of the *in vivo* assay is shown in Fig. 1.

Sample preparation

One day after the last tests, the rats were deeply anaesthetized with an overdose injection of sodium pentobarbitone (100 mg/kg, i.p., Simagchem, Xiamen, China) and sacrificed via decapitation. The L4-L6 segments of the spinal cord was collected. One half of the separated tissues were immediately stored in liquid nitrogen for further use, and the other half was fixed in 4% paraformaldehyde (Kemiou, Tianjin, China).

Microglia cells and treatment

Primary microglial cultures were isolated from neonatal rat spinal cords as described previously (Huang et al., 2016). Briefly, two-day old rats were euthanized, and the spinal cords were collected. The tissues were minced and incubated in 0.05% trypsin (Promega, USA). The dissociated cells were placed in Dulbecco's modified Eagle's medium (DMEM, Thermo Fisher Scientific, USA) containing 10% fetal bovine serum (FBS, Invitrogen, USA) and 1% penicillin (Quality Biological, USA). Cells were seeded in culture flasks for one week. Microglia cells were harvested by shaking for 4 h.

The rat immortalized microglia cell line HAPI was obtained from the China Center for Type Culture Collection (Wuhan, China) and cultured in DMEM supplemented with 10% fetal bovine serum and 1% penicillin.

To simulate hyperglycemic conditions, microglial cells were cultured in medium containing 30 mM glucose for 48 h. Medium containing 5.5 mM glucose served as the control.

In vitro transfection

Microglial cells were first plated in six-well plates at 2×10^5 cells/well. The transfection of lentiviral vector containing shRNA targeting TLR9 or negative shRNA was performed via the addition of lentiviral vectors (multiplicity of infection=10) to microglia culture for 48 h. The cells were washed using PBS, and the transfection efficiency was assessed using Western blotting.

Microglia viability detection

The viability of microglia was assessed using a Cell Counting Kit-8 (CCK-8) assay (Beyotime, Shanghai, China). Microglia with different treatments were incubated with 20 μl CCK-8 solution at 37°C for 2 h. The absorbance at a wavelength of 450 nm was measured using a microplate reader.

Microglia Chemotaxis Assay

The microglial chemotaxis assay was performed as described previously (Suzuki et al., 2011). Briefly, cells were incubated with 10 ng/mL IFN-γ (Sangon Biotech, China) for 24 h for activation. A 24-well chemotaxis plate with 8-μm pores (BD Biosciences, CA, USA) was used. Medium containing monocyte chemoattractant protein-1 (MCP-1, Sangon Biotech, China) was placed in the bottom wells, and cells with specific treatments were placed in the top wells. The incubation was maintained at 37°C for 4 h. The cells remaining in the top wells were removed using cotton swabs, and the cells in the bottom wells were photographed using light microscopy and manually counted.

Quantitative real-time PCR (qRT-PCR)

Total RNA from rat spinal cord and microglial cells was extracted using TRIzol reagent (Invitrogen, CA, USA) and quantified at 260 and 280 nm. The obtained RNA was reverse-transcribed using a PrimeScript RT Reagent kit (TaKaRa, Dalian, China) according to the manufacturer's instructions. qRT-PCR was performed using specific primers and SYBR Green (TaKaRa, Dalian, China), and the reaction program was set as described previously (Zhang et al., 2018a-c). The following primers were used in this study:

TLR9 (F: 5'-GAATGAGGACTGGGTGAGAAAC-3', R: 5'-CTCAGCAAGGACTTCTCCACTT-3'); GAPDH (F: 5'-TGAACGGGAAGCTCACTGG-3', R: 5'-GCTTCACCACCTTCTTGATGTC-3'); TNF-α (F: 5'-AGGACACCATGAGCACGGAA-3', R: 5'-GGGCCATGGAACTGATGAGA-3'); IL-1β (F: 5'-GCTGTCCAGATGAGAGCATC-3', R: 5'-GTCAGACAGCACGAGGCATT-3'); IL-6 (F: 5'-AGACTTCCAGCCAGTTGCCT-3', R: 5'-CTGACAGTGCATCATCGCTG-3'). The relative expression of genes was calculated using the $2^{-\Delta\Delta CT}$ method (Livak and Schmittgen, 2001), and GAPDH was selected as the reference gene.

Enzyme-linked Immunosorbent Assay (ELISA)

Measurement of proinflammatory cytokines in the rat spinal cord and culture medium supernatant was performed using commercial ELISA kits purchased from Sangon Biotech (Shanghai, China) in accordance with the manufacturer's instructions. The following ELISA kits were used: TNF-α (order No. D731168), IL-1β (order No. D731007), and IL-6 (order No. D731010). All absorbances were measured at a wavelength of 450 nm using a microplate reader (Bio-Tek, VT, USA).

Western Blotting

The protein of microglial cells and spinal cord was extracted at 4°C, and a BCA protein assay kit (Beyotime, Shanghai, China) was used for protein concentration quantification according to the manufacturer's instructions. The protein samples were

separated using 10% sodium dodecyl sulfate polyacrylamide gel electrophoresis (SDS-PAGE) and transferred to polyvinylidene difluoride (PVDF) membranes (Millipore, USA). After blocking with TBST containing 5% nonfat dry milk for 2 h, the membranes were incubated with specific primary and secondary antibodies at 4°C overnight. The following primary antibodies were used in this study: anti-TLR9 (rabbit monoclonal ab211012, 1:1000, Abcam, UK), anti-β-actin (mouse monoclonal ab6276, 1:5000, Abcam, UK), anti-p38 (rabbit monoclonal #8690, 1:1000, Cell Signaling Technology, USA), anti-p-p38 (rabbit monoclonal #4511, 1:1000, Cell Signaling Technology, USA), anti-ERK1/2 (rabbit monoclonal #4695, 1:1000, Cell Signaling Technology, USA), anti-p-ERK1/2 (rabbit monoclonal #4370, 1:2000, Cell Signaling Technology, USA), and anti-IBA-1 (rabbit monoclonal ab178846, 1:1000, Abcam, UK). Protein bands were visualized using an image analyzer (Bio-Rad, USA). The immunoblots were quantified using ImageJ software (version 1.53c, Bethesda, USA), and β-actin served as the internal reference.

Immunofluorescence Staining

Microglial cell and spinal cord sections were used for immunofluorescence analysis of a microglial activation marker, IBA-1. For spinal cord immunofluorescence, the detached spinal cords were fixed in 4% paraformaldehyde and incubated in 30% sucrose at 4°C overnight. Tissues were sliced into 20-μm thick sections and blocked with 10% goat serum (Solarbio, China) for 1 h. The sections were incubated with primary antibodies against IBA-1 (rabbit monoclonal ab178847, 1:100, Abcam, UK) at 4°C overnight followed by an Alexa 488-conjugated donkey anti-goat IgG secondary antibody (donkey polyclonal A-11055, 1:500; Thermo Fisher Scientific, USA) for 2 h at room temperature. Microglia cells were seeded on cover slips followed by incubation with 4% paraformaldehyde for 20 min at room temperature. The cells were rinsed using PBS. The cover slips were incubated with primary and secondary antibodies, and the nuclei were stained with DAPI (C1002, Beyotime Biotech, Shanghai, China). The immunofluorescence images were captured using a fluorescence microscope (Olympus, Tokyo, Japan).

Statistical Analysis

All of the results in this study were analyzed using Student's t test for comparisons between two groups, and ANOVA was used to determine statistical significance in multiple group comparisons. The Shapiro-Wilk test was used to check the normality of the data distribution. All data are presented as the means ± SD. A p-value <0.05 was considered statistically significant.

Results

TLR9 was up-regulated in a painful diabetic neuropathy rat model

Three weeks after STZ injection, body weights and blood glucose levels were detected. As indicated in Fig. 2A,B, body weights decreased dramatically in STZ injection rats compared to the sham group ($p<0.01$). Blood glucose levels were increased in the STZ group to a level two times the sham group ($p<0.01$). To evaluate the establishment of the painful diabetic neuropathy model, the rats were subjected to pain behavior measurements, including mechanical hypersensitivity and thermal hyperalgesia. The results in Fig. 2C,D show a significant reduction in pain threshold in the STZ group compared to the sham group ($p<0.01$).

The role of TLR9 was investigated in several diseases, including neuropathic pain and diabetes (David et al., 2013; Jiang and Chen, 2017; Luo et al., 2019). However, the role of TLR9 in the pathogenesis of painful diabetic neuropathy was not elucidated. We detected the expression of TLR9 in the spinal cord of painful diabetic neuropathy rats using qRT-PCR and Western blotting. As shown in Fig. 2E,F, the mRNA and protein levels of TLR9 were upregulated after STZ administration ($p<0.01$). These results suggest the involvement of TLR9 in painful diabetic neuropathy.

TLR9 knockdown suppressed hyperglycemia-induced microglial activation

The activation of microglia plays a vital role in the pathogenesis of painful diabetic neuropathy (Toth et al., 2010; Zhang et al., 2018a-c). Therefore, we determined whether high glucose induced the expression of TLR9 in microglia cells. Rat primary microglia and the immortalized microglial cell line HAPI were cultured in high glucose medium (30 mM) for 48 h. Stimulation with high glucose did not affect the viability of primary microglia and HAPI cells (Fig. 3A) ($p>0.05$). Thereafter, the expression of TLR9 was detected in the two microglia cultures, and an increase in TLR9 expression was observed at the mRNA and protein levels (Fig. 3B,C) ($p<0.01$), which was consistent with our results in the rat model. The results of TLR9 expression *in vivo* and *in vitro* suggest a role for TLR9 in painful diabetic neuropathy. To confirm this hypothesis, we knocked down TLR9 using two short hairpin RNAs in HAPI cells. The knockdown efficiency was determined using Western blotting (Fig. 3D). Inflammatory cytokine levels in microglial cells were detected using qRT-PCR and ELISA. As shown in Fig. 3E,F, the expression and secretion of TNF-α, IL-1β and IL-6 were dramatically induced under high glucose stimulation but suppressed by TLR9 interference ($p<0.01$). We also examined whether the depletion of TLR9 affected microglial chemotaxis. The results in Fig. 3G show that the

chemotactic response to MCP-1 was enhanced after high glucose stimulation, and this effect was reversed in microglial cells transfected with TLR9 shRNAs ($p<0.01$). We also evaluated the activation of microglia using IBA-1 immunofluorescence, which is a marker of activated microglia. IBA-1-positive microglia were increased in high glucose culture medium, but a decline in IBA-1-positive microglia was observed in the TLR9 knockdown group stimulated with high glucose (Fig. 3H) ($p<0.01$). These results suggest that TLR9 contributes to high glucose stimulation-induced microglia activation.

TLR9 participates in the hyperglycemia-induced activation of the p38 MAPK pathway in microglia

Previous studies reported that the activation of p38 MAPK was closely related to the pathogenesis of hyperalgesia (Wu et al., 2011; Moon et al., 2013) and the activation of microglia (Zhuang et al., 2007). Therefore, we determined whether the TLR9 expression induced by high glucose stimulation affected p38 MAPK signal activation. As indicated in Fig. 4A, culture with high glucose markedly activated the p38 MAPK pathway in microglial cells, which was assessed by the increase in phospho-p38 and phospho-ERK1/2, but total p38 and ERK1/2 levels remained largely unchanged ($p<0.01$). The inhibition of TLR9 using shRNA interference partially abrogated the high glucose-induced p38 MAPK hyperactivation. Because TLR9 contributes to the activation of p38 MAPK, we further evaluated the role of p38 MAPK in hyperalgesia-induced microglial activation. We treated microglial cells with a widely used p38 inhibitor, SB203580 (20 μM) (Sun et al., 2017), to block the p38 MAPK pathway. The results in Fig. 4B suggest that SB203580 had a strong inhibitory effect on p38 MAPK activation but failed to alter TLR9 abundance ($p<0.01$). Inflammatory cytokines were suppressed to varying degrees after SB203580 administration (Fig. 4C) ($p<0.01$) SB203580 also limited microglial chemotaxis, but to a lesser extent than TLR9 interference (Fig. 4D) ($p<0.01$). We also detected the effect of SB203580 on IBA-1 expression using immunofluorescence, and SB203580 administration reduced IBA-1 expression ($p<0.01$) (Fig. 4E). Therefore, our data revealed that p38 MAPK was in a critical downstream pathway of TLR9, and TLR9 inhibition reduced high glucose-induced microglial activation at least partially via deactivation of the p38 MAPK pathway.

Knockdown of TLR9 mitigates hyperalgesia in painful diabetic neuropathy rats

RNA interference via lentiviral delivery in laboratory animals has shed new light on the treatment of some nervous system disorders, such as neuropathic pain and Alzheimer's disease (Singer et al., 2005; Jia et al., 2019). The present study observed a crucial role of TLR9 in high glucose-induced microglial activation *in*

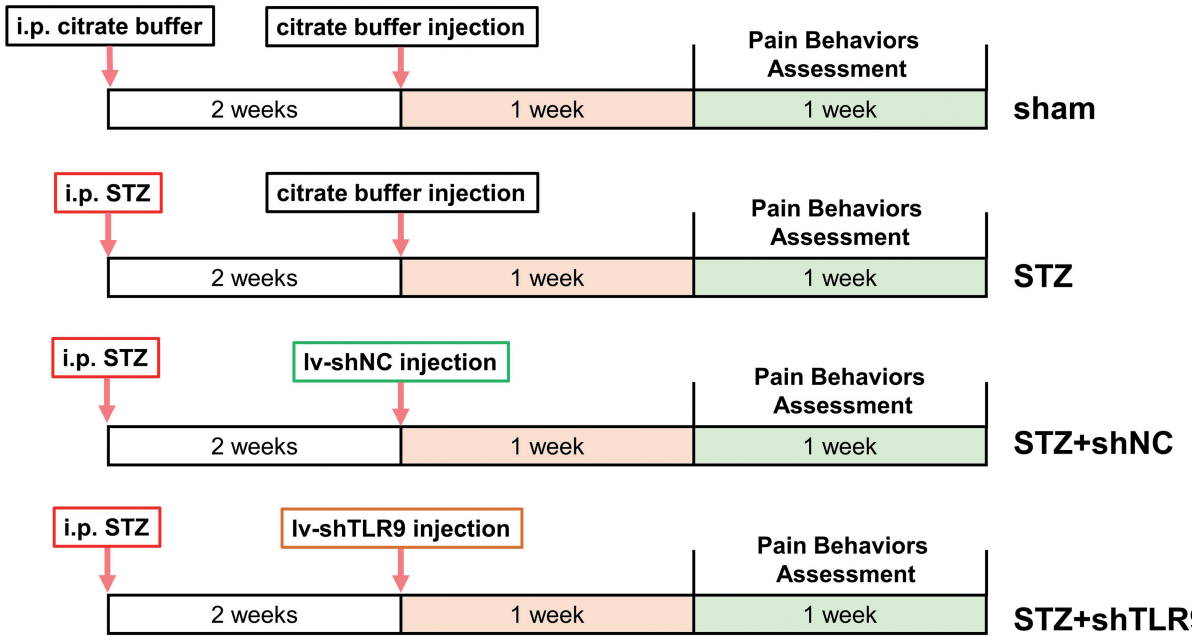

Fig. 1. The timeline of the *in vivo* assay. Rats in each group (n=48, 12 per group) received i.p. streptozotocin (STZ) or an equal volume of citrate buffer. After two weeks, rats were injected with citrate buffer or the indicated lentivirus particles. Pain behaviors were assessed one week after lentivirus injection.

vitro. We also determined the role of TLR9 *in vivo* using lentivirus-mediated TLR9 knockdown. The lentivirus was delivered to the rat spinal cord two weeks after STZ injection, and pain behaviors were tested 21 days after STZ injection. STZ injection induced significant mechanical and thermal hyperalgesia, as assessed by the reductions in mechanical withdrawal thresholds (MWT) and paw withdrawal latency (PWL), respectively, and depletion of TLR9 partially alleviated mechanical and thermal hyperalgesia (Fig. 5A,B) ($p<0.01$). TLR9 knockdown also suppressed STZ-induce microglia activation as shown by the decrease in IBA-1 immunofluorescence (Fig. 5C, upper) and protein content (Fig. 5C, lower) ($p<0.01$). The STZ-induced elevation of inflammatory cytokine secretion (TNF-α, IL-1β and IL-6) was decreased in the presence of lentiviral-mediated TLR9 knockdown (Fig. 5D) ($p<0.01$). shRNA interference and MAPK pathway activation blocked the increase in TLR9 protein (Fig. 5E) ($p<0.01$). In conclusion, TLR9 knockdown relieved painful diabetic neuropathy in a rat model, likely via deactivation of the MAPK pathways.

Discussion

Diabetes mellitus (DM) is an endocrine and metabolic disorder caused by insulin secretory deficiency or insulin resistance, and the principal manifestation is high blood glucose. Patients with sustained chronic hyperglycemia largely develop some chronic complications, such as diabetic retinopathy, diabetic nephropathy, and diabetic neuropathy.

A large number of recent studies demonstrated that glia also played an important role in the pathogenesis and development of peripheral neuropathy. Glial activation was investigated in various animal nervous system disorder models, including nerve injury and hyperalgesia (Zhang and De Konink, 2006; Sato et al., 2014). Microglia are glial cells that play vital roles in the immune response in the central nervous system. They primarily exist in the brain and spinal cord and account for approximately 20% of glia (Fu et al., 2014). Active microglia in the nervous system express cell-surface molecules, such as CD11b, and secrete some chemical mediators, including proinflammatory cytokines (Tsuda et al., 2005). Previous studies found that pain and other noxious stimuli altered the activity of microglia-related receptors and led to abnormal activation. Activation increases the release of signaling molecules, which directly or indirectly act on neuropathic neurons and result in the amplification of pain signals (Tsuda et al., 2005). Numerous reports elucidated genes and pathways that were implicated in the activation of microglia in pain disorders. For example, the expression of $P2X_7R$

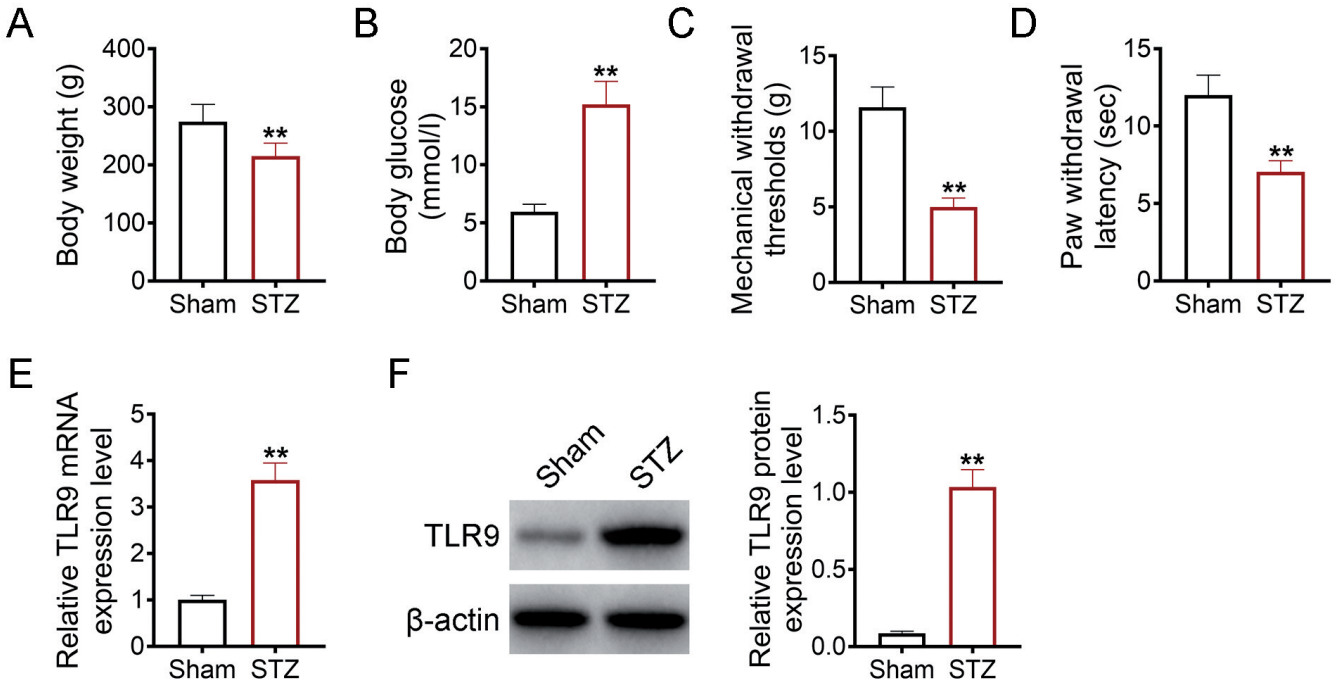

Fig. 2. The establishment of a painful diabetic neuropathy model in rats. Rats received a single intraperitoneal injection of STZ, and blood glucose levels after 72 h were used to evaluate the induction of hyperglycemia. The rats were continually fed for 3 weeks, and body weight **(A)** and blood glucose **(B)** were measured. Von Frey filaments **(C)** were used to examine mechanical hypersensitivity, and thermal hyperalgesia **(D)** was evaluated using the laser radiant method. The mRNA **(E)** and protein **(F)** expression levels were detected in the rat spinal cord. Data are presented as the means ± SD. **$p<0.01$. Student's t test was used for comparisons between two groups.

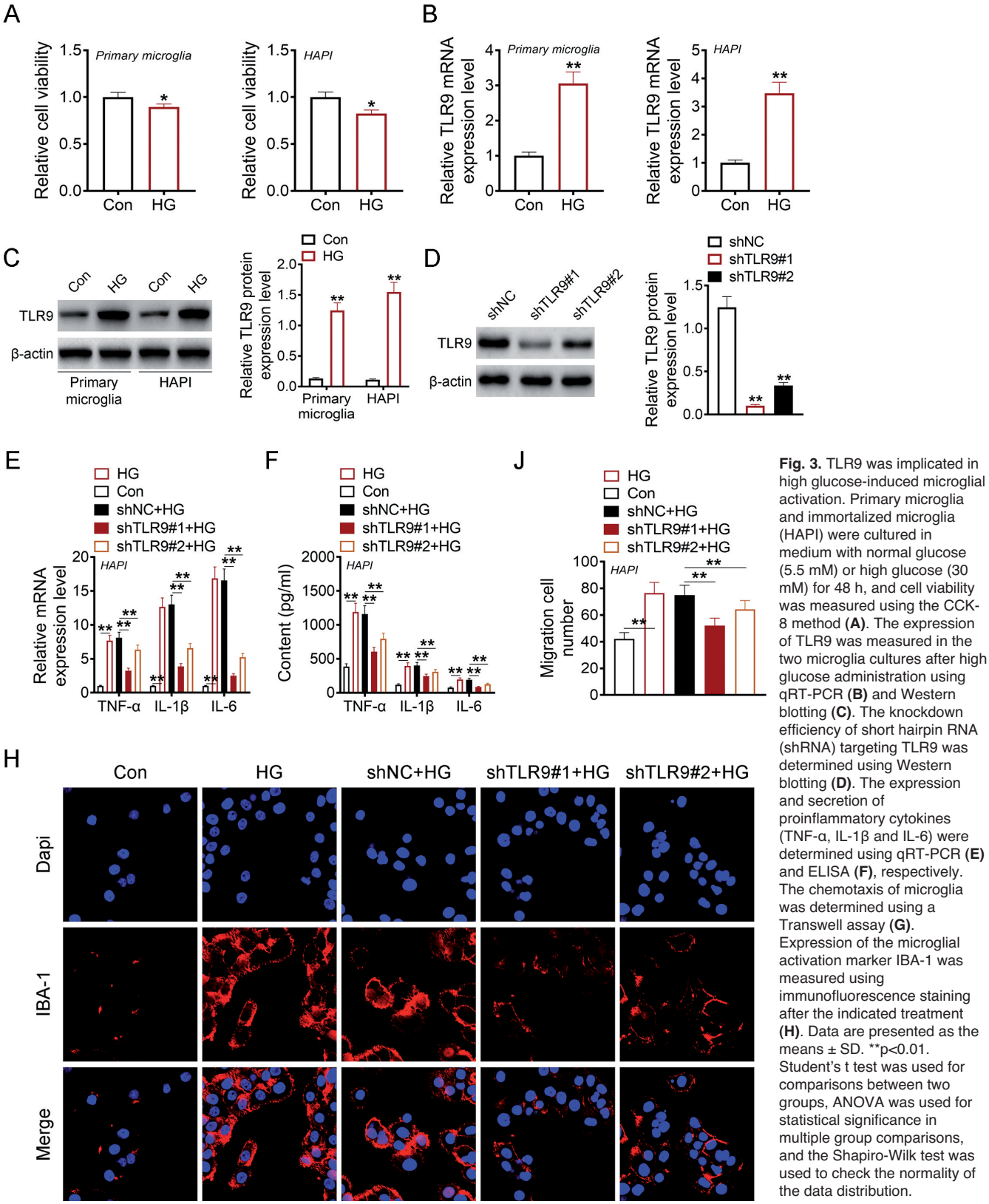

Fig. 3. TLR9 was implicated in high glucose-induced microglial activation. Primary microglia and immortalized microglia (HAPI) were cultured in medium with normal glucose (5.5 mM) or high glucose (30 mM) for 48 h, and cell viability was measured using the CCK-8 method **(A)**. The expression of TLR9 was measured in the two microglia cultures after high glucose administration using qRT-PCR **(B)** and Western blotting **(C)**. The knockdown efficiency of short hairpin RNA (shRNA) targeting TLR9 was determined using Western blotting **(D)**. The expression and secretion of proinflammatory cytokines (TNF-α, IL-1β and IL-6) were determined using qRT-PCR **(E)** and ELISA **(F)**, respectively. The chemotaxis of microglia was determined using a Transwell assay **(G)**. Expression of the microglial activation marker IBA-1 was measured using immunofluorescence staining after the indicated treatment **(H)**. Data are presented as the means ± SD. **p<0.01. Student's t test was used for comparisons between two groups, ANOVA was used for statistical significance in multiple group comparisons, and the Shapiro-Wilk test was used to check the normality of the data distribution.

was induced in spinal microglia, and a $P2X_7R$ antagonist relieved mechanical allodynia and thermal hypersensitivity in a neuropathic pain model by suppressing microglial activation (He et al., 2012). Spinal nerve-induced NADPH oxidase 2 promotes ROS generation and microglial activation, which subsequently contribute to pain hypersensitivity (Kim et al., 2010). Inhibition of P2Y12 overexpression in dorsal horn microglia alleviated neuropathic pain, and downstream GTP-RhoA/ROCK2 signaling was identified (Yu et al., 2019). Our study observed enhanced expression of TLR9 in the spinal cord after induction of painful diabetic neuropathy, and our further experiments demonstrated the participation of TLR9 in hyperglycemia-induced spinal microglial activation *in vitro* and *in vivo*. Notably, an upregulation of TLR9 was observed in retinas of rats with diabetic retinopathy (Jiang and Chen, 2017). The involvement of TLR9 was recently clarified in high blood glucose-induced diabetic encephalopathy, and TLR9 knockout or inhibition lowered β-amyloid deposition and tau hyperphosphorylation in the hippocampus (Sun et al., 2017). These data suggest a vital role of TLR9 in some diabetes-induced complications, especially nervous system disorders. Most notably, recent evidence demonstrated that TLR9 targeting may be a potential

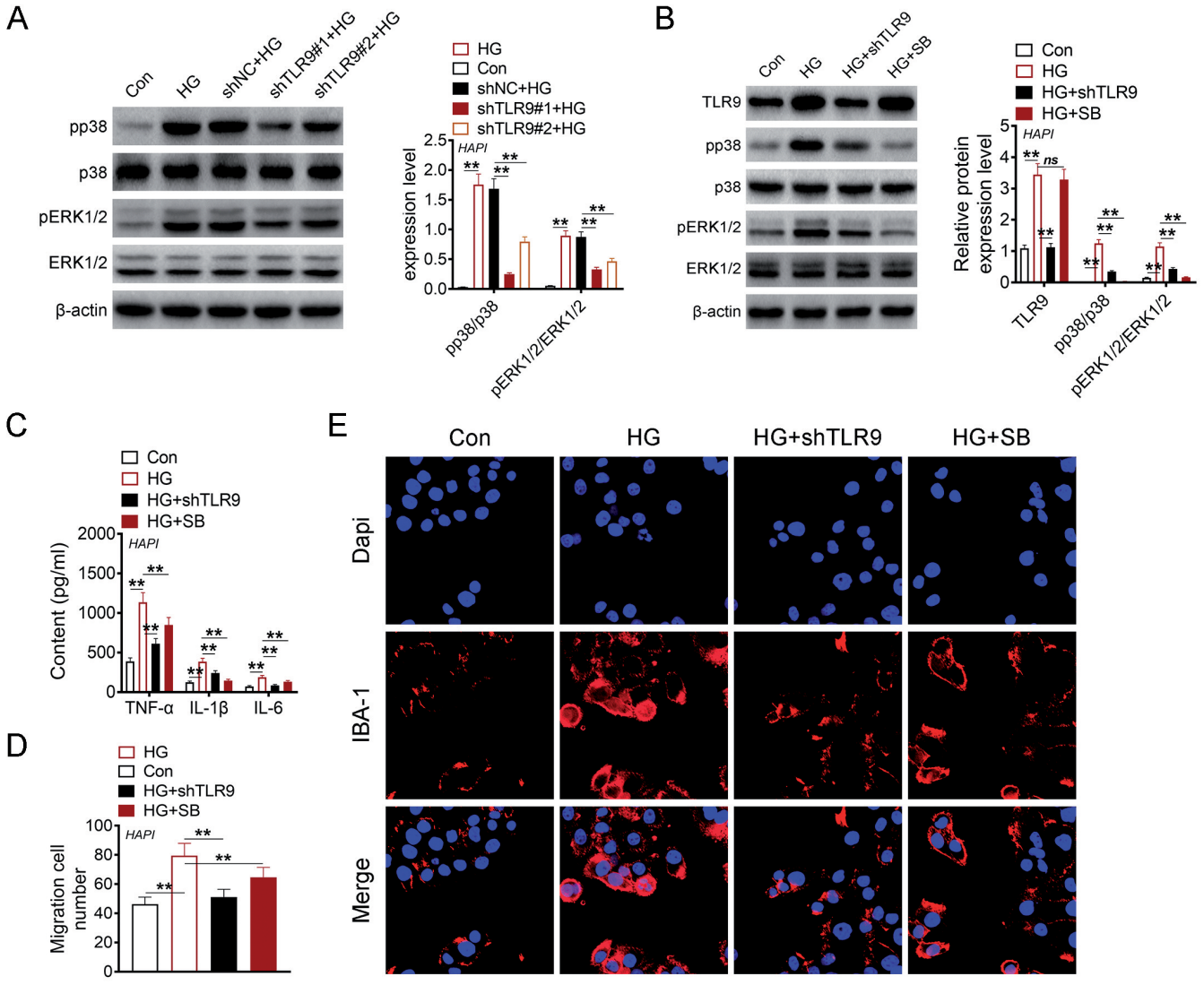

Fig. 4. TLR9 interference inhibited activation of the MAPK pathway. The proteins involved in the MAPK pathway (pp38, p38, pERK1/2, and ERK1/2) were determined using Western blotting **(A, B)** after different treatments. SB represents the p38 inhibitor SB203580. Proinflammatory cytokine secretion **(C)**, chemotaxis **(D)** and IBA-1 **(E)** expression in microglia treated with shTLR9 or SB203580 in the presence of high glucose. Data are presented as the means ± SD. **p<0.01. ANOVA was used to determine statistical significance in multiple group comparisons, and the Shapiro-Wilk test was used to check the normality of the data distribution.

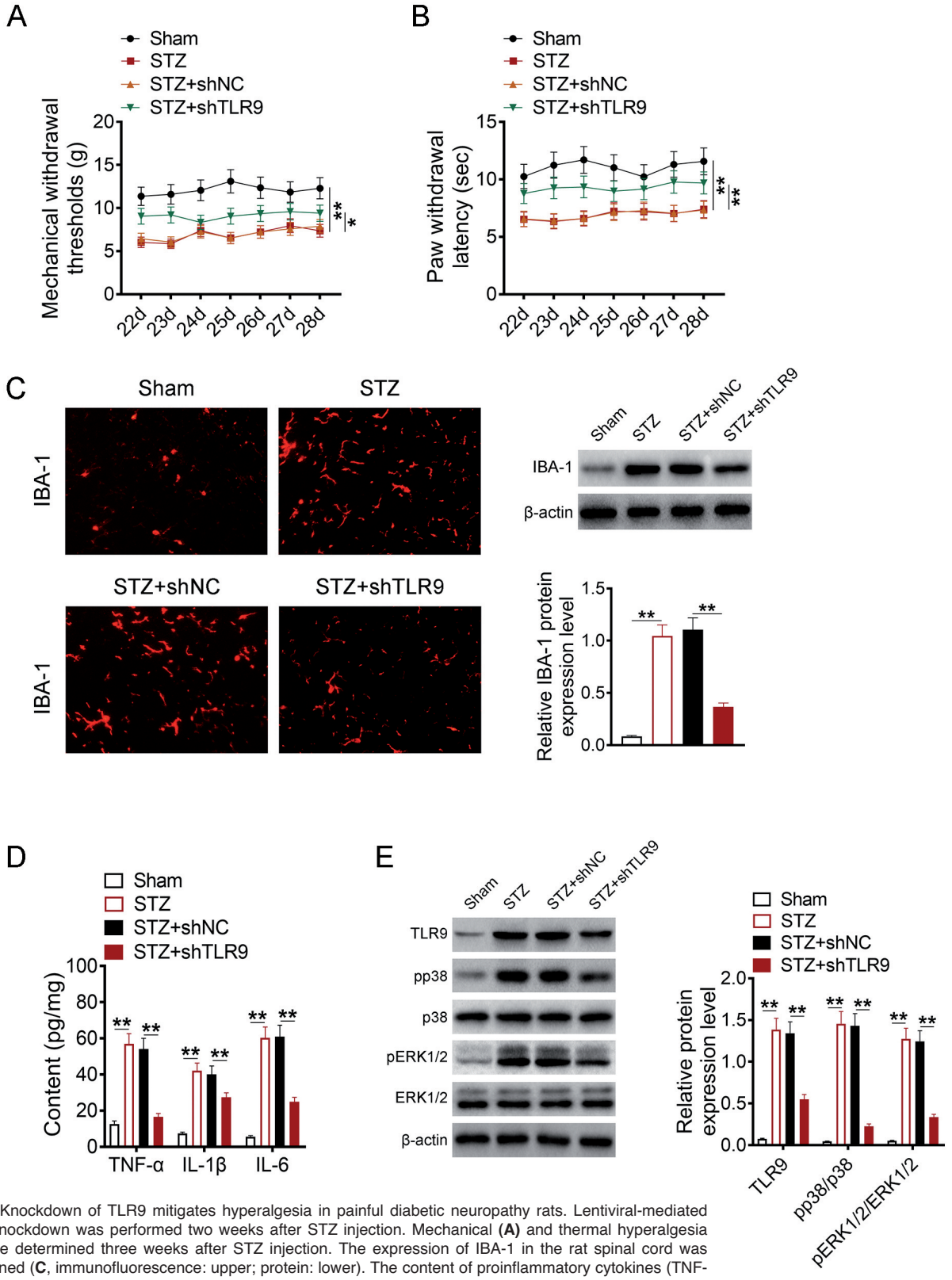

Fig. 5. Knockdown of TLR9 mitigates hyperalgesia in painful diabetic neuropathy rats. Lentiviral-mediated TLR9 knockdown was performed two weeks after STZ injection. Mechanical **(A)** and thermal hyperalgesia **(B)** were determined three weeks after STZ injection. The expression of IBA-1 in the rat spinal cord was determined (**C**, immunofluorescence: upper; protein: lower). The content of proinflammatory cytokines (TNF-α, IL-1β and IL-6) **(D)** and protein abundance (TLR9, pp38, p38, pERK1/2, and ERK1/2) in the rat spinal cord **(E)**. Data are presented as the means ± SD. **p<0.01. ANOVA was used to determine the statistical significance in multiple group comparisons, and the Shapiro-Wilk test was used to check the normality of the data distribution.

strategy for the treatment of neuropathic pain. A Toll-like receptor 9 antagonist reduced spinal cord injury-induced hyperalgesia (David et al., 2013). Recent research revealed that paclitaxel-induced mechanical allodynia led to the infiltration of macrophages into dorsal root ganglia but was not affected by TLR9 mutation. However, TLR9 mutation or inhibitors virtually reduced paclitaxel-induced mechanical allodynia, and this effect varied by sex (Luo et al., 2019).

MAPK signaling activation contributes to the pathogenesis of some pain disorders. Aberrant activation of MAPK signaling was widely investigated in neuropathic pain and other chronic pain (Lin et al., 2014). The inhibition of MAPK in pain hypersensitivity also produced a significant effect (Ma and Quirion, 2005; Smith et al., 2013; Zhou et al., 2016). Our study observed MAPK activation in a painful diabetic neuropathy rat model and high glucose-treated microglia. The inhibitory effect on microglial activation following MAPK blockade was clarified in some previous research (Zhuang et al., 2007). Our study further demonstrated that the knockdown of TLR9 abolished the hyperglycemia-induced activation of MAPK signaling. The role of high glucose-induced TLR9-p38 MAPK was elucidated in neurons, which led to neuronal apoptosis (Sun et al., 2017).

In summary, our results implicate TLR9-MAPK signaling in high glucose-induced microglial activation and the pathogenesis of painful diabetic neuropathy. The inhibition of TLR9 also alleviated painful diabetic neuropathy, which further supports the therapeutic value of TLR9 targeting in the treatment of some pain disorders.

References

Castany S., Carcolé M., Leánez S. and Pol O. (2016). The induction of heme oxygenase 1 decreases painful diabetic neuropathy and enhances the antinociceptive effects of morphine in diabetic mice. PLoS One, 11, e0146427.

David B.T., Ratnayake A., Amarante M.A., Reddy N.P., Dong W., Sampath S., Heary R.F. and Elkabes S. (2013). A toll-like receptor 9 antagonist reduces pain hypersensitivity and the inflammatory response in spinal cord injury. Neurobiol. Dis. 54, 194-205.

Ebata-Kogure N., Nozawa K., Murakami A., Toyoda T., Haga Y. and Fujii K. (2017). Clinical and economic burdens experienced by patients with painful diabetic peripheral neuropathy: An observational study using a Japanese claims database. PLoS One 12, e0187250.

Fu R., Shen Q., Xu P., Luo J.J. and Tang, Y. (2014). Phagocytosis of microglia in the central nervous system diseases. Mol. Neurobiol. 49, 1422-1434.

He W.-J., Cui J., Du L., Zhao Y.-D., Burnstock G., Zhou H.-D. and Ruan H.-Z. (2012). Spinal P2X7 receptor mediates microglia activation-induced neuropathic pain in the sciatic nerve injury rat model. Behav. Brain Res. 226, 163-170.

Huang Q., Mao X.-F., Wu H.-Y., Li T.-F., Sun M.-L., Liu H. and Wang Y.-X. (2016). Bullatine A stimulates spinal microglial dynorphin A expression to produce anti-hypersensitivity in a variety of rat pain models. J. Neuroinflammation 13, 1-18.

Jia L., Zhang Y., Qu Y.J., Huai J., Wei H. and Yue S.W. (2019). Gene therapy by lentivirus-mediated RNA interference targeting extracellular-regulated kinase alleviates neuropathic pain *in vivo*. J. Cell. Biochem. 120, 8110-8119.

Jiang S. and Chen X. (2017). Expression of high-mobility group box 1 protein (HMGB1) and toll-like receptor 9 (TLR9) in retinas of diabetic rats. Med. Sci. Monit. 23, 3115-3122.

Kim D., You B., Jo E.-K., Han S.-K., Simon M.I. and Lee S.J. (2010). NADPH oxidase 2-derived reactive oxygen species in spinal cord microglia contribute to peripheral nerve injury-induced neuropathic pain. Proc. Natl. Acad. Sci. USA 107, 14851-14856.

Lin X., Wang M., Zhang J. and Xu R. (2014). p38 MAPK: A potential target of chronic pain. Curr. Med. Chem. 21, 4405-4418.

Lin J.-y., He Y.-n., Zhu N. and Peng B. (2018). Metformin attenuates increase of synaptic number in the rat spinal dorsal horn with painful diabetic neuropathy induced by type 2 diabetes: a stereological study. Neurochem. Res. 43, 2232-2239.

Livak K.J. and Schmittgen T.D. (2001). Analysis of relative gene expression data using real-time quantitative PCR and the 2– ΔΔCT method. Methods 25, 402-408.

Luo X., Huh Y., Bang S., He Q., Zhang L., Matsuda M. and Ji R.-R. (2019). Macrophage toll-like receptor 9 contributes to chemotherapy-induced neuropathic pain in male mice. J. Neurosci. 39, 6848-6864.

Ma W. and Quirion R. (2005). The ERK/MAPK pathway, as a target for the treatment of neuropathic pain. Expert Opin. Ther. Targets, 9, 699-713.

Maruta T., Nemoto T., Hidaka K., Koshida T., Shirasaka T., Yanagita T., Takeya R. and Tsuneyoshi I. (2019). Upregulation of ERK phosphorylation in rat dorsal root ganglion neurons contributes to oxaliplatin-induced chronic neuropathic pain. PLoS One 14, e0225586.

Moon J.-Y., Roh D.-H., Yoon S.-Y., Kang S.-Y., Choi S.-R., Kwon S.-G., Choi H.-S., Han H.-J., Beitz A.J. and Lee J.-H. (2013). Sigma-1 receptor-mediated increase in spinal p38 MAPK phosphorylation leads to the induction of mechanical allodynia in mice and neuropathic rats. Exp. Neurol. 247, 383-391.

Morrow T.J. (2004). Animal models of painful diabetic neuropathy: the STZ rat model. Curr. Protoc. Neurosci. 29, 9-18.

Nasiry D., Ahmadvand H., Amiri F.T. and Akbari E. (2017). Protective effects of methanolic extract of *Juglans regia* L. leaf on streptozotocin-induced diabetic peripheral neuropathy in rats. BMC Complement. Altern. Med. 17, 476.

Oghbaei H., Mohaddes G., Hamidian G. and Keyhanmanesh R. (2020). Sodium nitrate preconditioning prevents progression of the neuropathic pain in streptozotocin-induced diabetes Wistar rats. J. Diabetes Metab. Disord. 19, 105.

Oka T., Hikoso S., Yamaguchi O., Taneike M., Takeda T., Tamai T., Oyabu J., Murakawa T., Nakayama H., Nishida K., Akira S., Yamamoto A. and Nishida, K. (2012). Mitochondrial DNA that escapes from autophagy causes inflammation and heart failure. Nature 485, 251-255.

Sato K.L., Johanek L.M., Sanada L.S. and Sluka K.A. (2014). Spinal cord stimulation reduces mechanical hyperalgesia and glial cell activation in animals with neuropathic pain. Anesth. Analg. 118, 464.

Shintani Y., Kapoor A., Kaneko M., Smolenski R.T., D'Acquisto F., Coppen S.R., Harada-Shoji N., Lee H.J., Thiemermann C.,

Takashima S., Yashiro K. and Suzuko K. (2013). TLR9 mediates cellular protection by modulating energy metabolism in cardiomyocytes and neurons. Proc. Natl. Acad. Sci. USA 110, 5109-5114.

Silver A.C., Arjona A., Walker W.E. and Fikrig E. (2012). The circadian clock controls toll-like receptor 9-mediated innate and adaptive immunity. Immunity 36, 251-261.

Singer O., Marr R.A., Rockenstein E., Crews L., Coufal N.G., Gage F.H., Verma I.M. and Masliah E. (2005). Targeting BACE1 with siRNAs ameliorates Alzheimer disease neuropathology in a transgenic model. Nat. Neurosci. 8, 1343-1349.

Sloan G., Shillo P., Selvarajah D., Wu J., Wilkinson I.D., Tracey I., Anand P. and Tesfaye S. (2018). A new look at painful diabetic neuropathy. Diabetes Res. Clin. Pract. 144, 177-191.

Smith M.T., Woodruff T.M., Wyse B.D., Muralidharan A. and Walther T. (2013). A small molecule angiotensin II type 2 receptor (AT2R) antagonist produces analgesia in a rat model of neuropathic pain by inhibition of p38 mitogen-activated protein kinase (MAPK) and p44/p42 MAPK activation in the dorsal root ganglia. Pain Med. 14, 1557-1568.

Sun Y., Xiao Q., Luo C., Zhao Y., Pu D., Zhao K., Chen J., Wang M. and Liao Z. (2017). High-glucose induces tau hyperphosphorylation through activation of TLR9-P38MAPK pathway. Exp. Cell Res. 359, 312-318.

Suzuki N., Hasegawa-Moriyama M., Takahashi Y., Kamikubo Y., Sakurai T. and Inada E. (2011). Lidocaine attenuates the development of diabetic-induced tactile allodynia by inhibiting microglial activation. Anesth. Analg. 113, 941-946.

Toth C.C., Jedrzejewski N.M., Ellis C.L. and Frey W.H. (2010). Cannabinoid-mediated modulation of neuropathic pain and microglial accumulation in a model of murine type I diabetic peripheral neuropathic pain. Mol. Pain 6, 16-22.

Tsuda M., Inoue K. and Salter M.W. (2005). Neuropathic pain and spinal microglia: a big problem from molecules in 'small'glia. Trends Neurosci. 28, 101-107.

Tsuda M., Ueno H., Kataoka A., Tozaki-Saitoh H. and Inoue K. (2008). Activation of dorsal horn microglia contributes to diabetes-induced tactile allodynia via extracellular signal-regulated protein kinase signaling. Glia 56, 378-386.

Wang D., Couture R. and Hong Y. (2014). Activated microglia in the spinal cord underlies diabetic neuropathic pain. Eur. J. Pharmacol. 728, 59-66.

Wickramasinghe T.P., Subasinghe S., Withana A.K.G. and Wellala D.A.H. (2016). Prevalence, burden and treatment response of diabetic peripheral neuropathy among attendees of the Diabetic Clinic in the Sri Jayewardenepura General Hospital. J. Ceylon Coll. Physicians 47

Wu J., Xu Y., Pu S., Jiang W. and Du D. (2011). p38/MAPK inhibitor modulates the expression of dorsal horn GABA (B) receptors in the spinal nerve ligation model of neuropathic pain. Neuroimmunomodulation 18, 150-155.

Yu T., Zhang X., Shi H., Tian J., Sun L., Hu X. Cui W. and Du D. (2019). P2Y12 regulates microglia activation and excitatory synaptic transmission in spinal lamina II neurons during neuropathic pain in rodents. Cell Death Dis. 10, 1-16.

Zhang J. and De Koninck Y. (2006). Spatial and temporal relationship between monocyte chemoattractant protein-1 expression and spinal glial activation following peripheral nerve injury. J. Neurochem., 97, 772-783.

Zhang T.-T., Xue R., Fan S.-Y., Fan Q.-Y., An L., Li J., Zhu L., Ran Y.-H., Zhang L.-M., Zhong B.-H., Li Y.-F., Ye C.-Y. and Zhang Y.-Z. (2018a). Ammoxetine attenuates diabetic neuropathic pain through inhibiting microglial activation and neuroinflammation in the spinal cord. J. Neuroinflammation 15, 1-13.

Zhang T.-T., Xue R., Fan S.-Y., Fan Q.-Y., An L., Li J., Zhu L., Ran Y.-H., Zhang L.-M., Zhong B.-H., Li Y.-F., Ye C.-Y. and Zhang Y.-Z. (2018b). Ammoxetine attenuates diabetic neuropathic pain through inhibiting microglial activation and neuroinflammation in the spinal cord. J. Neuroinflammation 15, 1-13.

Zhang Z., Qin P., Deng Y., Ma Z., Guo H., Guo H., Hou Y., Wang S., Zou W., Sun Y. Ma Y. and Hou W. (2018c). The novel estrogenic receptor GPR30 alleviates ischemic injury by inhibiting TLR4-mediated microglial inflammation. J. Neuroinflammation 15, 206.

Zhong Y., Huang Y.-L., Hu Y.-M., Zhu L.-R. and Zhao Y.-S. (2018). Puerarin alleviate radicular pain from lumbar disc herniation by inhibiting ERK-dependent spinal microglia activation. Neuropeptides 72, 30-37.

Zhou J., Wang L., Wang J., Wang C., Yang Z., Wang C., Zhu Y. and Zhang J. (2016). Paeoniflorin and albiflorin attenuate neuropathic pain via MAPK pathway in chronic constriction injury rats. Evid. Based Complement. Alternat. Med. 2016

Zhuang Z.-Y., Kawasaki Y., Tan P.-H., Wen Y.-R., Huang J. and Ji R.-R. (2007). Role of the CX3CR1/p38 MAPK pathway in spinal microglia for the development of neuropathic pain following nerve injury-induced cleavage of fractalkine. Brain Behav. Immun. 21, 642-651.

Accepted December 10, 2021